## 5.1. McMurdo Station (02/09/04 – 1/25/05)

The 2004/05 season at McMurdo Station is defined as the period between the site visits 2/2/04 – 2/11/04 and 1/24/05 – 2/1/05. The season opening and closing calibrations were performed on 2/6/04 and 1/25/05, respectively. Volume 14 solar data comprises the period 02/09/04 – 1/25/05. About 96% of the scheduled scans are part of the data set; less than 1% are missing because of technical problems.

The brightness of the internal reference lamp showed a comparatively larger drift throughout the year. In addition, an abrupt change of 7% was observed on 11/9/04. We have seen similar drifts with other lamps of this type recently and attribute those to quality problems of the lamps, which are beyond our control. These drifts were corrected by adjusting the instrument's calibration accordingly and the effect on published solar data is therefore small.

The Eppley PSP and TUVR instruments installed at McMurdo were replaced by identical instruments during the site visit in 2004. We generally cannot confirm the calibrations provided by Eppley Laboratory Inc. and therefore advise data users to treat TUVR data as "uncalibrated," and use them for referential purposes only.

### 5.1.1. Irradiance Calibration

The site irradiance standards for the McMurdo 2004/05 season were the lamps 200W005, 200W019, and M-543. Lamp M-764 was used as traveling standard. Its calibration was established by Optronic Laboratories in March 2001. Lamps 200W005 and M-543 were recalibrated by comparison with M-764 using scans performed during the site visits in 2001 and 2002 (see Section 4.2.1.5 for details of the procedure). Lamp 200W019 has an Optronic Laboratories certificate from September 1998, and was not recalibrated.

Figure 5.1.1 shows the Volume 14 season opening calibrations performed on 2/6/04. All standards agreed at the ±1.0% level. A similar comparison for measurements performed at the end of the season (1/25/05) is shown in Figure 5.1.2. Two additional comparisons between M-543, 200W005, and 200W019 performed mid-season (on 5/3/04 and 8/18/04) indicated a similar level of agreement.

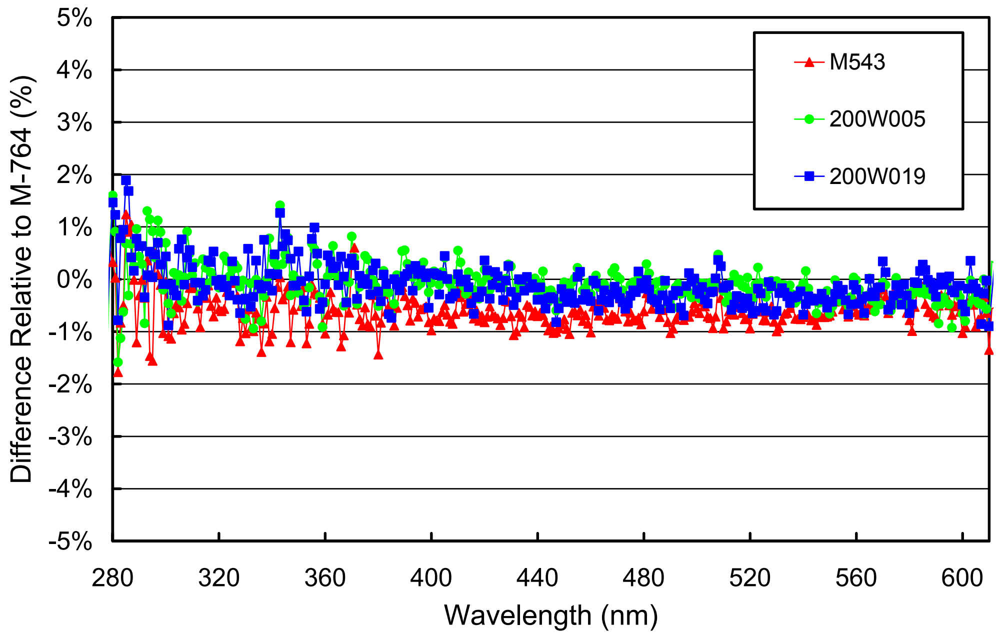


**Figure 5.1.1.** *Comparison of McMurdo lamps M-543, 200W005, and 200W019 with the BSI traveling standard M-764 at the beginning of the season (2/6/04).*

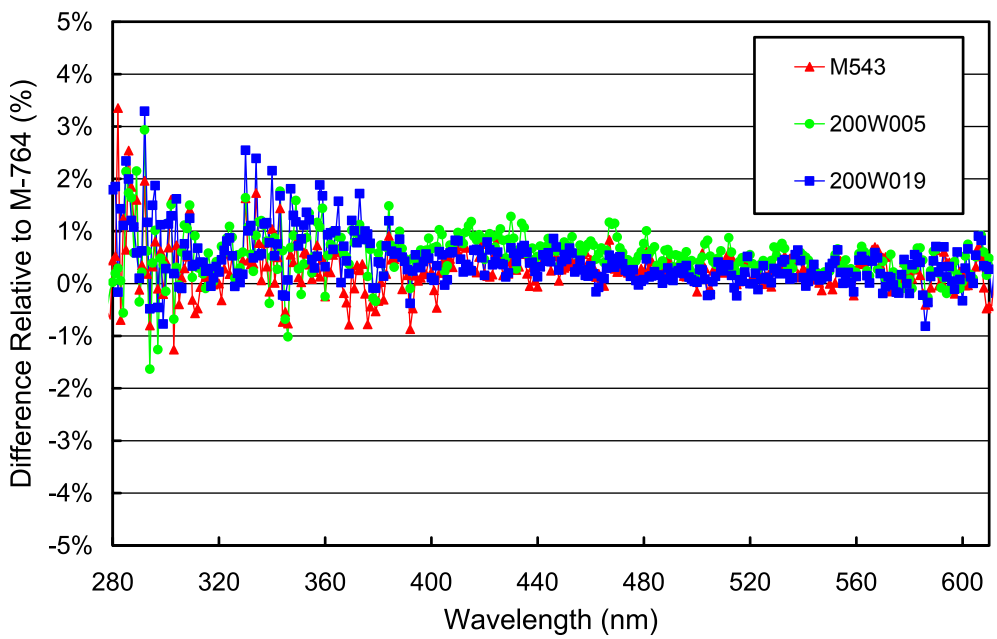


**Figure 5.1.2.** *Comparison of McMurdo lamps M-543, 200W005, and 200W019 with the BSI traveling standard M-764 at the end of the season (1/25/05).*

### 5.1.2. Instrument Stability

The stability of the spectroradiometer over time is primarily monitored with bi-weekly calibrations utilizing the site irradiance standards and daily response scans of the internal irradiance reference lamp. The stability of this lamp is monitored with the TSI sensor, which is independent from possible monochromator and PMT drifts. By logging the PMT currents at several wavelengths during response scans, changes in monochromator throughput and PMT sensitivity can be detected.

Figure 5.1.3 shows the changes in TSI readings and PMT currents at 300 and 400 nm, derived from the daily response scans. TSI measurements indicate that the internal reference lamp became brighter by approximately 10% between the start of the season and 11/9/04. On the following day, the reference lamp's brightness decreased abruptly by about 7% and remained unstable during the following week. The lamp remained fairly stable during the remainder of the season. The change in PMT currents tracked the change in TSI readings fairly well, indicating that most of the variability was related to the reference lamp.

The season was broken in eight calibration periods to correct for the change of irradiance of the internal lamp. In each of these periods, a different irradiance function was assigned to this lamp following the procedure outlined in Section 4.2.1.2. Figure 5.1.4 shows the ratios of those functions relative to the function applied in the first period (02/06/04 – 04/04/04). An overview of the calibration periods is given in Table 5.1.1. Solar data between 11/9/04 and 11/18/04 were "paired" with the scan of the internal executed on 11/9/04. Thus, the system was "made to believe" that the lamp was stable during the period of large instability. The procedure is acceptable since we do not have indications that other components (e.g. monochromator, PMT) were unstable during this period. Calibrated data also compare well with measurements of the collocated GUV-511 radiometer (Section 5.1.5).

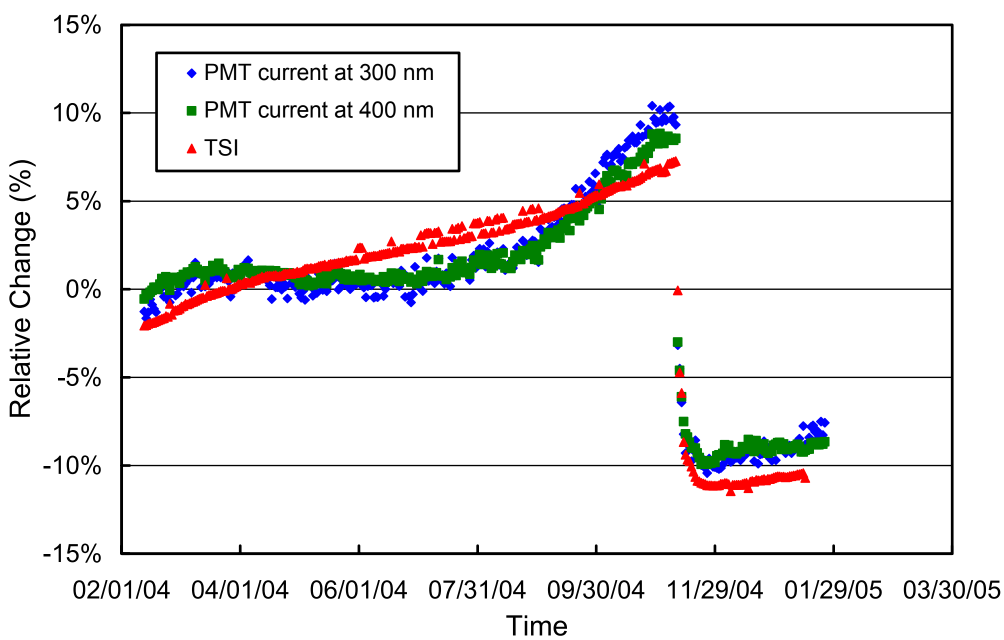


**Figure 5.1.3.** *Time-series of PMT current at 300 and 400 nm, and TSI signal during measurements of the internal irradiance reference lamp during the McMurdo 2004/05 season. Data are normalized to the average value of the whole season.*

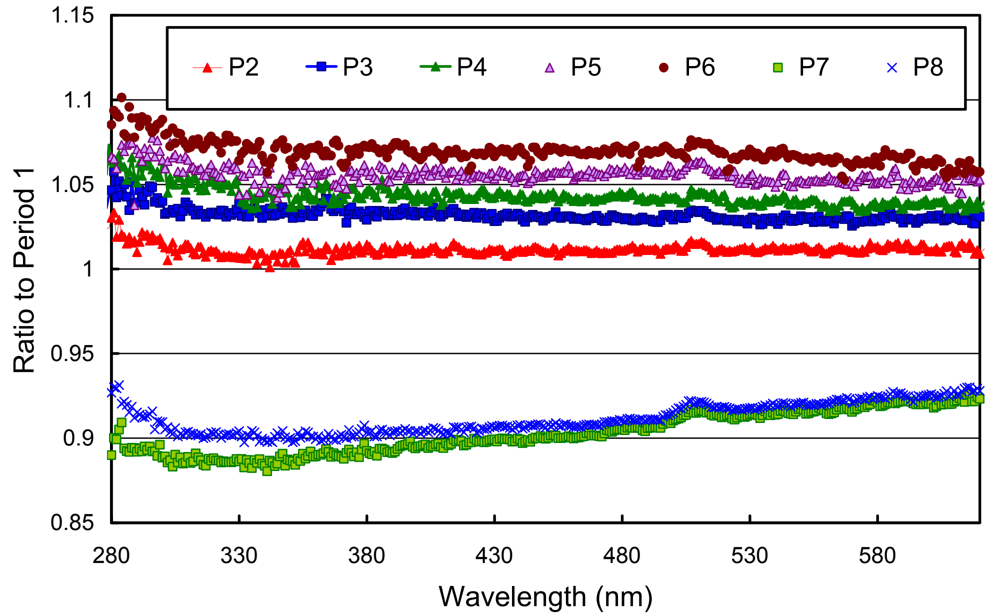


**Figure 5.1.4** *Ratio of irradiance assigned to the internal reference lamp to Period 1.*

Figure 5.1.5 presents the ratios of the standard deviation and average spectra, calculated from the individual absolute scans of those periods that include more than two calibration scans. These ratios are useful for estimating the variability of the calibrations in each period. The variability is typically less than 1% for wavelengths above 300 nm in all periods, indicating good consistency of absolute scans performed in each period.

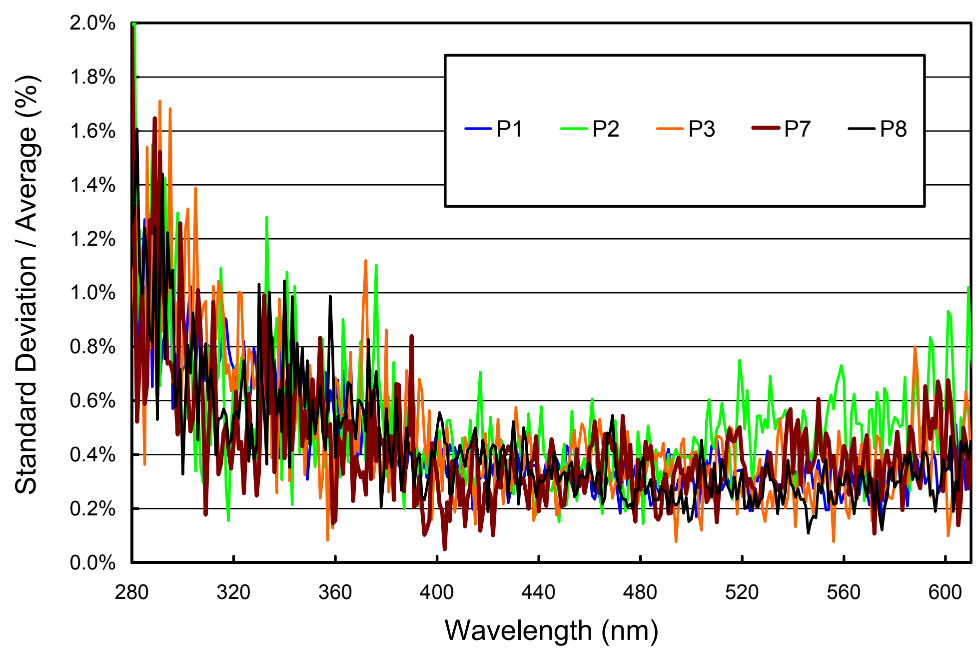


**Figure 5.1.5.** *Ratio of standard deviation and average calculated from the absolute calibration scans.*

**Table 5.1.1: Calibration periods of McMurdo Volume 14 data.**

| Period name | Period range | Number of Absolute scans | Remarks |
|---|---|---|---|
| P1 | 02/06/04 - 04/04/04 | 11 | |
| P2 | 04/05/04 - 06/20/04 | 4 | Before Polar Night |
| P3 | 06/21/04 - 09/10/04 | 4 | After Polar Night |
| P4 | 09/11/04 - 10/06/04 | 2 | |
| P5 | 10/07/04 - 10/21/04 | 1 | |
| P6 | 10/22/04 - 11/18/04 | 2 | Includes unstable period |
| P7 | 11/19/04 - 01/20/05 | 3 | |
| P8 | 01/21/05 - 01/25/05 | 8 | |

### 5.1.3. Wavelength Calibration

Wavelength stability of the system was monitored with the internal mercury lamp. Information from the daily wavelength scans was used to homogenize the data set by correcting day-to-day fluctuations in the wavelength offset. After this step, there may still be a deviation from the correct wavelength scale, but this bias should ideally be the same for all days. Figure 5.1.6 shows the differences in the wavelength offset of the 296.73 nm mercury line between two consecutive wavelength scans. In total, 395 pairs of scans were evaluated. For 86% of the days, the offset change was smaller than ±0.025 nm; for 96% of the days it was smaller than ±0.055 nm. The wavelength difference between two consecutive scans was larger than 0.1 nm and data from these days were adjusted accordingly.

After the data were corrected for day-to-day wavelength fluctuations, the wavelength-dependent bias between this homogenized data set and the correct wavelength scale was determined with the Fraunhofer-correlation method, as described in Section 4.2.2.2. The correction function is shown in Figure 5.1.7. After the data was wavelength corrected using this function, the wavelength accuracy was again tested with the Fraunhofer method. The results are shown in Figure 5.1.8 for four UV wavelengths. For UV wavelengths lower than 320 nm or higher than 390 nm, the residual shifts are typically smaller than ±0.1 nm. For wavelengths between 320 and 390 nm, residual shifts can be as high as ±0.17 nm. This value is comparatively high and an indication of higher-than-usual fluctuations in the monochromator's wavelength mapping function. The increased variability is difficult to correct. Wavelength shifts in the UVA of this magnitude are fortunately of little consequence for most applications. Only if spectra are compared on a wavelength-by-wavelength basis, a discernible scatter may be observed. Figure 5.1.8 also indicates enhanced scatter at 310 nm shortly before and after polar night. This is due to small solar irradiance levels during this part of the year. The wavelength stability is not worse during this time; yet the correction algorithm is less precise.

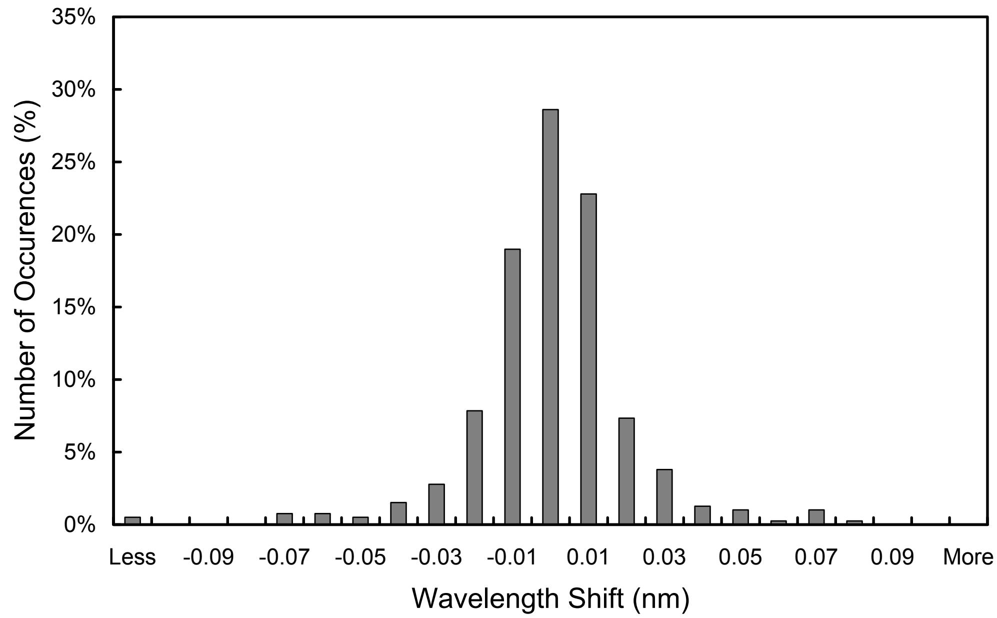


**Figure 5.1.6.** *Differences in the measured position of the 296.73 nm mercury line between consecutive wavelength scans. The x-labels give the center wavelength shift for each column. The 0-nm histogram column covers the range -0.005 to +0.005 nm. "Less" means shifts smaller than –0.105 nm; "more" means shifts larger than 0.105 nm.*

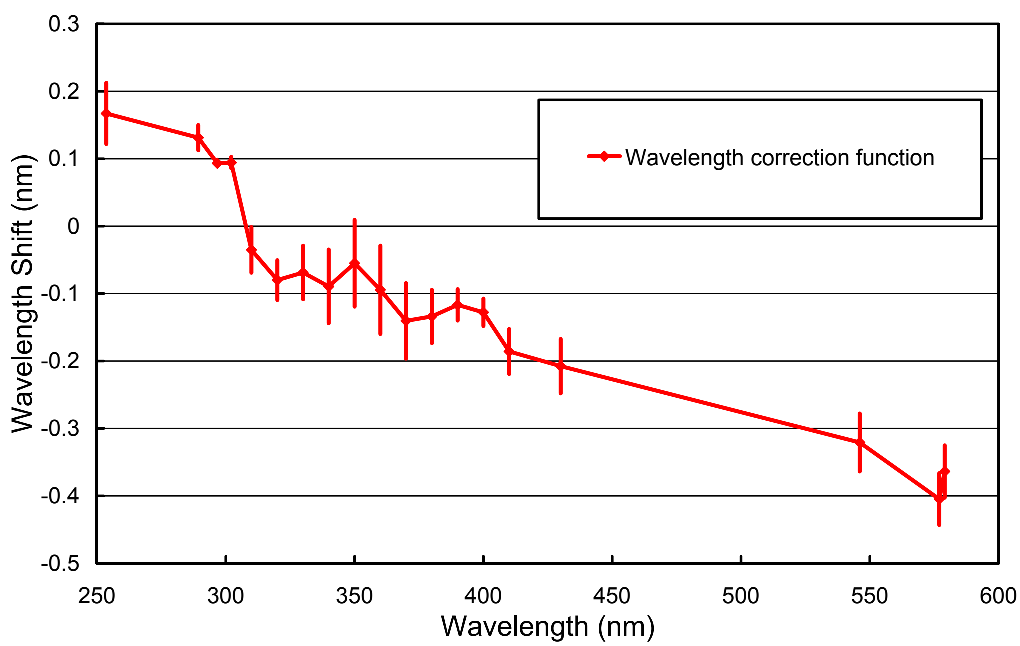


**Figure 5.1.7.** *Monochromator non-linearity correction functions for McMurdo 2004/05 data.*

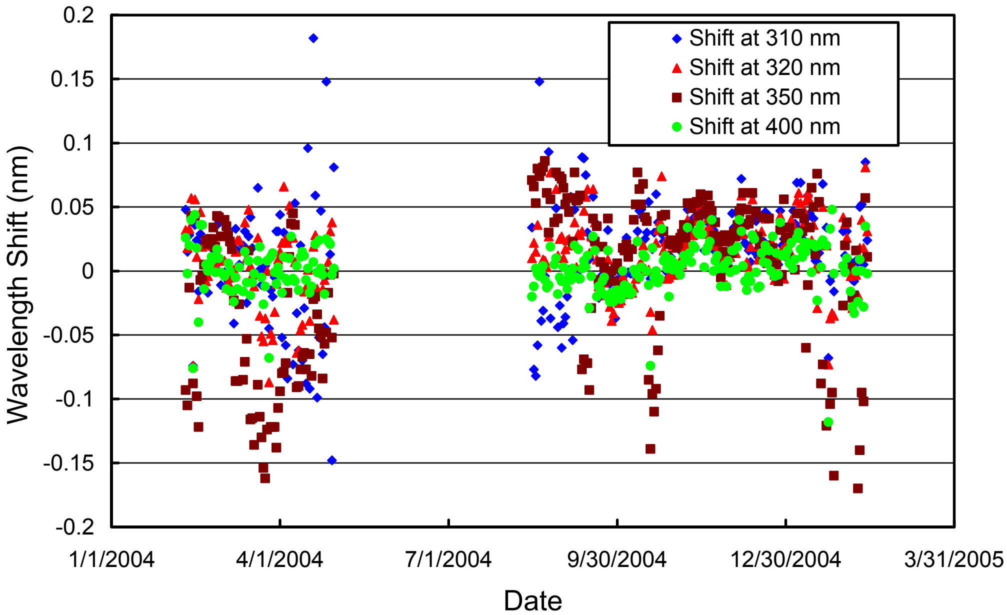


**Figure 5.1.8.** *Check of the wavelength accuracy of final data at four wavelengths by means of Fraunhofer correlation. The noontime measurement has been evaluated for each day of the season. No correlation data is available during Polar Night.*

Data from the external mercury scans do not have a direct influence on data products. They are, however, an important part of instrument characterization. Figure 5.1.9 illustrates the difference between internal and external mercury scans collected during both site visits. The wavelength scale of the figure is the same as applied during solar measurements. The peak of the external scans agrees well with the nominal wavelength of 296.73 nm, whereas the peak of the internal scans is shifted about 0.08 nm to shorter wavelengths. External scans have a bandwidth of about 1.01 nm FWHM. The bandwidth of the internal scan is 0.74 nm. Since external scans have the same light path as solar measurements, they represent the monochromator bandpass relevant for solar scans in the UV-B. Scans at start and end of the season are very consistent.

## 5.1.4. Missing Data

A total of 16664 scans are part of the published McMurdo Volume 14 dataset. These are 95.7% of the scans scheduled. Of all missing data scans, 111, 230, and 271 were superseded by absolute, wavelength, and response scans, respectively. Approximately 0.7% of all scans were missed due to technical problems: 42 scans were not recorded on 3/1/04 for reasons unknown. 23 scans are missing on 8/25/04 and 8/26/04 also for reasons unknown. In addition, 53 scans measured at various times are missing from the period 8/12/04 – 9/15/04.

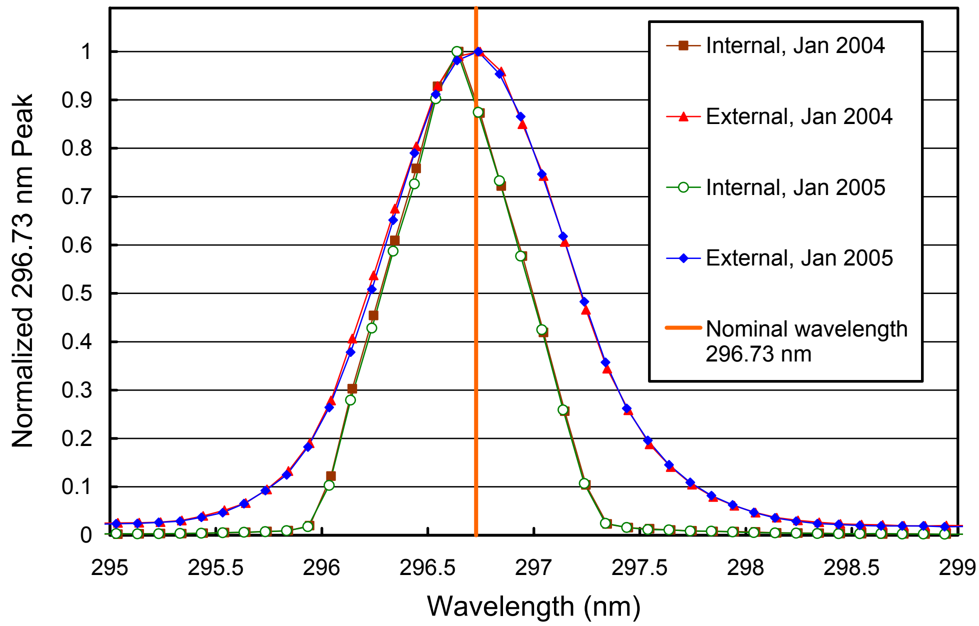


**Figure 5.1.9** *The 296.73 mercury line as registered by the PMT from external and internal sources. The wavelength scale is the same as applied for solar measurements, i.e., it is based on a combination of internal scans and the Fraunhofer-correlation method. It is assumed that the wavelength registration of the monochromator did not shift between internal and external scans, which were close in time.*

### 5.1.5. GUV Data

The GUV-511 radiometer was installed next to the SUV-100 and calibrated against final SUV-100 measurements following the procedure outlined in Section 4.3.1. Data products were calculated from the calibrated measurements (Section 4.3.2). Figure 5.1.10. shows a comparison of GUV-511 and SUV-100 erythemal irradiance based on final Volume 14 data. For SZA smaller than 80°, 99% of the data agree to within ±10% with each other.

The agreement for some data products (e.g. DNA damaging variation) may be worse than that for erythema due to principal limitations in calculating dose-rates from the four GUV-511 channels when the Sun is low and when the data product in question is heavily weighted toward wavelengths below 310 nm. We therefore advise data users to use SUV-100 rather than GUV-511 data when possible, in particular for low-Sun conditions.

Note that a new data set of SUV-100 data, named “Version 2” is currently in preparation (see http://www.biospherical.com/nsf/Version2/Version2.asp). Version 2 data are corrected for the cosine error of the SUV-100 spectroradiometer. Version 2 erythemal data are approximately 6% higher than the Version 0 data that are discussed in this report. GUV measurements were calibrated both against cosine error corrected and uncorrected SUV-100 data, and both data sets were published. Preliminary GUV data made available via the website http://www.biospherical.com/nsf/login/update.asp are based on the calibration with the cosine corrected SUV-100 data set, and are therefore approximately 6% higher than data plotted in Figure 5.1.10.

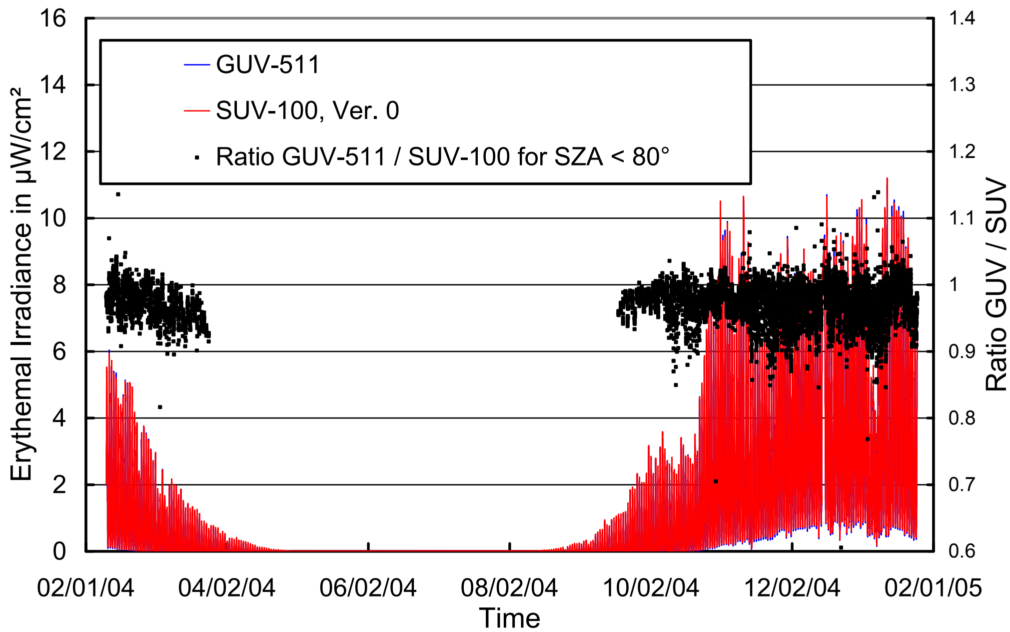


**Figure 5.1.10.** *Comparison of erythemal irradiance measured by the SUV-100 spectroradiometer and the GUV-511 radiometer. All data is based on "Version 0" (cosine-error uncorrected) data, see text.*

Figure 5.1.11 shows a comparison of total ozone measurements from the GUV-511 and NASA/TOMS Earth Probe satellite (Version 8). GUV-511 ozone values were calculated following the procedure outlined in Section 4.3.3. TOMS ozone values are on average 4% smaller than GUV-511 data. For SZA larger than 85°, GUV-511 data become unreliable and should not be used.

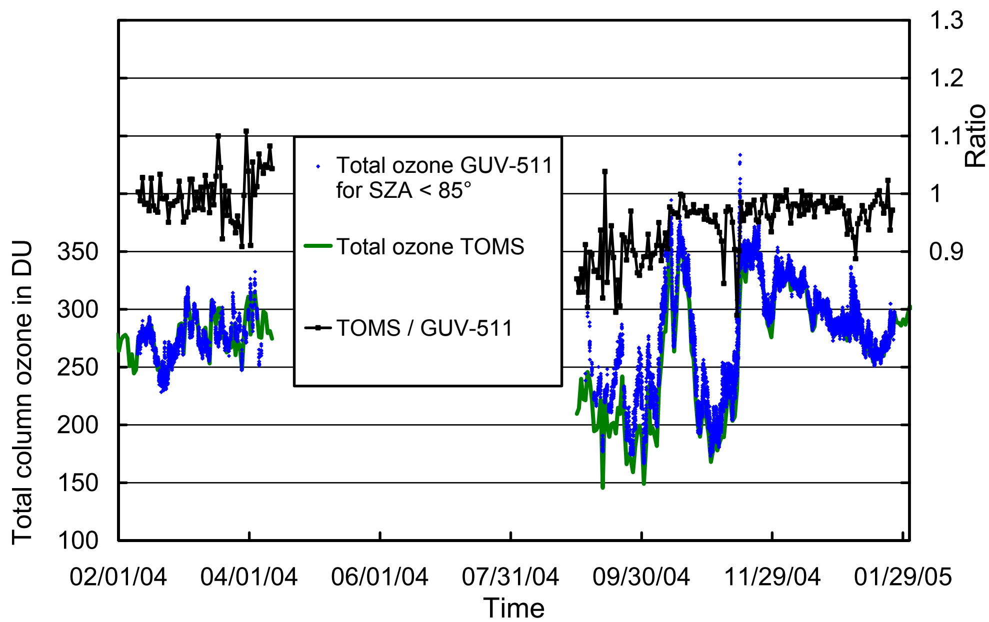


**Figure 5.1.11.** *Comparison of total column ozone measurements from GUV-511 and NASA/TOMS Earth Probe satellite. GUV-511 measurements are plotted in 15 minute intervals. For calculating the ratio of both data sets, only GUV-511 measurements concurrent with the TOMS overpass data were evaluated.*